

# DC Side Ripple Voltage Analysis and Fuzzy PI Control Strategy Research for APF

Ting Wu, Jian-Feng Yang and Qing Miao\*

Lanzhou Jiao Tong University, Lanzhou, Gansu, 730070, China

**Abstract:** Owing to the problems of DC side capacitor value choice in the application of Active Power Filter (APF), this article presents a technique based on the analysis of the ripple voltage in DC side by graining appropriately the undulation control rate within the range of settings and control DC voltage so that the voltage fluctuation rate can reach minimum value under the condition of specific capacitance which is aimed at getting good compensation effects. In order to achieve the stability of the DC side capacitor voltage control, we introduce a new technique on the DC output voltage deviation square values of adaptive fuzzy PI control. Meanwhile, a Space Vector Pulse Width Modulation (SVPWM) is used to conduct optimization design for the DC side voltage waveform. The simulation results show that using this method reduces the DC voltage ripple and achieves steady DC output voltage.

**Keywords:** DC side ripple voltage, Active Power Filter (APF), New PI control, Space Vector Pulse Width Modulation (SVPWM).

## 1. INTRODUCTION

Active Power Filter (APF) is highly controllable and responsive. It can not only compensate harmonics but also inhibit flicker and react power compensation [1, 2]. However, due to time-varying in compensation current and the inverter's own consumption as well as its failure, an appropriate control measures need to be taken to avoid DC capacitor voltage decay or occurrence of large fluctuations, not all but also, accompanying large number of ripples which may occur in APF [3, 4]. In fact, stability of voltage across the capacitor in DC side of APF has significant impact on APF compensation performance [5-7]. Therefore its ripple voltage should be controlled carefully within permissible range. Several factors have impacts on the ripple voltage such as the frequency of compensation current, effective value of source voltage, DC voltage across the capacitor and so on. In most cases, the capacitance needs to be determined according to the range of ripple voltages. After reading a lot of the relevant literature, we find few people research on the ripple voltage on the DC side. For example, in the literature [8-12], the authors mentioned it but they did not specify a solution.

In this paper we put forward a fuzzy-PI control of a new DC-side output voltage deviation squared value which uses the DC voltage deviation squared value  $\Delta U_{dc}^2$  as the input of fuzzy PI control. This method has the following advantages:

- Effectively reduces the no-load current

- Improves on both ends of the dc side voltage rise time and
- Improves the dynamic characteristic of the system

In addition to SVPWM pulse width modulation, a lot of reviewed literature mostly adopted SPWM modulation or PWM adjustment. But however, this paper verifies the latter by simulation and experiment.

## 2. THE ANALYSIS OF APF DC SIDE RIPPLE VOLTAGE

Fig. (1) depicts a system block diagram of the APF in which  $e_a, e_b,$  and  $e_c$  are APF access phase supply voltage grids;  $i_a, i_b$  and  $i_c$  are three-phase power supply currents;  $i_{ca}, i_{cb}$  and  $i_{cc}$  are the required compensation currents;  $i_{la}, i_{lb}$  and  $i_{lc}$  are the load currents; C is the DC side capacitance;  $u_{dc}$  and  $i_{dc}$  are the voltage and current flowing through capacitor respectively, and L is a inductor [13-15].

Three-phase shunt active filter APF is obtained from Fig. (1) and the AC side voltage is three-phase current equation:

$$\begin{cases} e_a - u_a = L \frac{di_a}{dt} \\ e_b - u_b = L \frac{di_b}{dt} \\ e_c - u_c = L \frac{di_c}{dt} \\ i_a + i_b + i_c = 0 \end{cases} \quad (1)$$

\*Address correspondence to this author at the Lanzhou Jiao tong University, Lanzhou, Gansu, 730070, China; Tel: 18894011612; E-mail: 18894011612@163.com

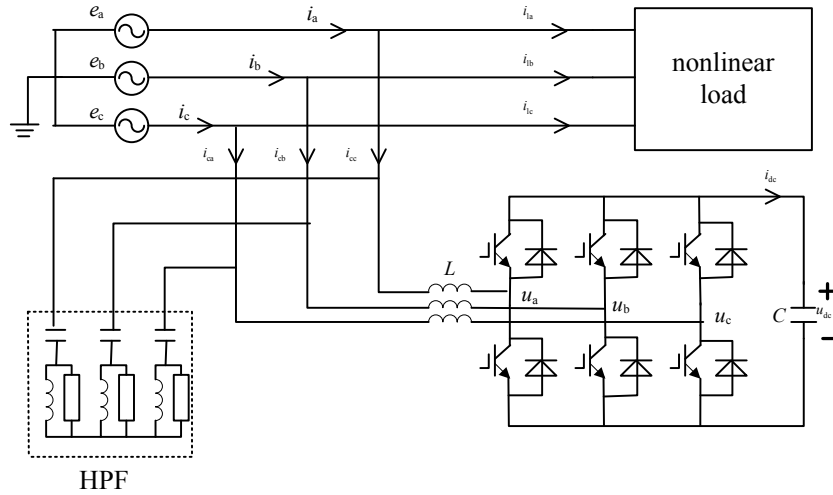


Fig. (1). APF system structure.

Set  $k_a$ ,  $k_b$  and  $k_c$  as the inverter switching functions and  $k_{i[a,b,c]}$  is defined as:

$$k_i = \begin{cases} 1 & \text{tube closed on and disconnect the down tube} \\ 0 & \text{disconnect the pipe and closed down tube} \end{cases} \quad (2)$$

Wherein a, b, c are three inverter bridge arm APF. Bridge work alternately open arms off, but the steady-state operation can be APF inverter input voltage and current of the DC side, which is expressed as:

$$\begin{cases} u_a = k_a \frac{u_{dc}}{2} \\ u_b = k_b \frac{u_{dc}}{2} \\ u_c = k_c \frac{u_{dc}}{2} \\ i_d = i_a \frac{k_a + 1}{2} + i_b \frac{k_b + 1}{2} + i_c \frac{k_c + 1}{2} \end{cases} \quad (3)$$

Putting equations (1) and (2) into equation (3), the DC side current can be expressed as:

$$i_d = \frac{1}{u_{dc}} \left[ M - \frac{L}{2} \cdot \frac{dN}{dt} \right] \quad (4)$$

The formula:

$$M = e_a i_a + e_b i_b + e_c i_c \sqrt{b^2 - 4ac}, \quad N = i_a^2 + i_b^2 + i_c^2$$

Considering the DC capacitor voltage and current relationship, we have:

$$u_{dc} = \sqrt{\frac{2W}{C} + \frac{2}{C} \cdot \int_0^t M dt \frac{LN}{C}} \quad (5)$$

Where W can be taken as an arbitrary constant which indicates the initial energy stored in DC capacitor.

As seen from equation (5),  $2W/c$  is the constant term whereas  $\frac{2}{C} \cdot \int_0^t M dt \frac{LN}{C}$  is the integral term and a function

of time representing the DC capacitor voltage fluctuations. When the three-phase grid voltage is balanced and without distortion, we have:

$$\begin{cases} e_a = E_m \sin \omega t \\ e_b = E_m \sin(\omega t - 120^\circ) \\ e_c = E_m \sin(\omega t + 240^\circ) \end{cases} \quad (6)$$

Regardless of the compensation current is symmetrical or not, compensation current can be decomposed into:

$$\begin{cases} i_a = \sum i_{an} = \sum [i_{an}^+ + i_{an}^- + i_{an}^0] \\ i_b = \sum i_{bn} = \sum [i_{bn}^+ + i_{bn}^- + i_{bn}^0] \\ i_c = \sum i_{cn} = \sum [i_{cn}^+ + i_{cn}^- + i_{cn}^0] \end{cases} \quad (7)$$

The formula:  $n=1,3,5,7,9,11,13,15,17,19$ .  $i_{an}^+, i_{bn}^+, i_{cn}^+, i_{an}^-, i_{bn}^-, i_{cn}^-, i_{an}^0, i_{bn}^0, i_{cn}^0$  shows the corresponding phase sequence, n denotes harmonic currents of positive sequence components and negative sequence components and zero sequence components.

Joining equations (5) and (6), vertical DC side ripple voltage can be obtained as follows:

$$u_{dc} = \sqrt{\frac{2W}{C} + \mathfrak{U} + \mathfrak{Q}} \quad (8)$$

Where:  $\mathfrak{U} = -\frac{3L}{2C} \sum_{n \neq 3m} [(I_n^+)^2 + (I_n^-)^2]$

$$\mathfrak{Q} = \frac{-3E_m}{\omega C} \sum_{n \neq 3m} \left\{ \frac{I_n^+}{n+1} \sin[(n+1)\omega t + \varphi_n^-] - \frac{I_n^+}{n-1} \sin[(n-1)\omega t + \varphi_n^+] \right\}$$

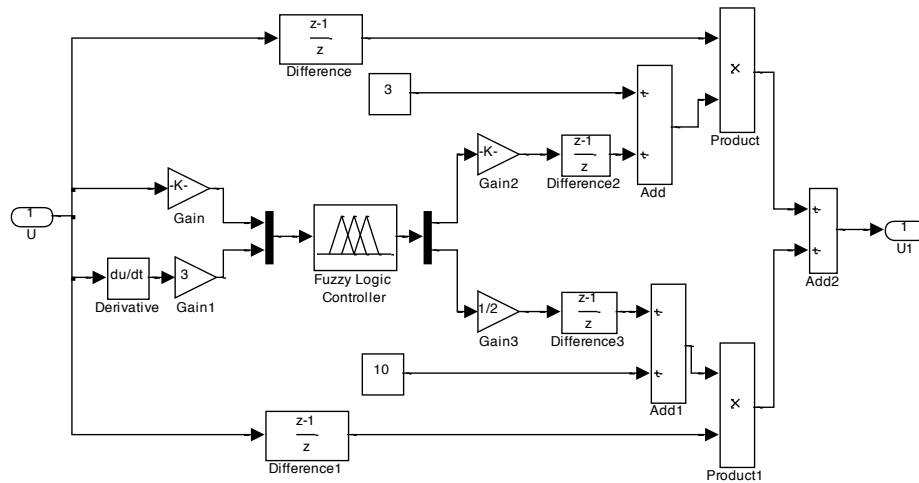


Fig. (2). Fuzzy PI control.

$$\Omega_2 = \frac{3L}{C} \left\{ \sum_{\substack{h < k \\ h, k \neq 3m}} \left\{ I_h^+ I_k^+ \cos[(h-k)\omega t + \varphi^+ - \varphi_{kh}^-] - I_h^- I_k^- \cos[(h-k)\omega t + \varphi_h^+ - \varphi_k^-] \right\} - \sum_{\substack{h \geq k \\ h, k \neq 3m}} \left\{ I_h^+ I_k^- \cos[(h+k)\omega t + \varphi_h^+ + \varphi_k^-] \right\} \right\}$$

Assuming that compensated nonlinear load is a large inductive load on the uncontrolled rectifier bridge of the DC side, then the phase current on dc side is given by:

$$i_a = \frac{2\sqrt{3}}{\pi} I_d \left[ \sin \omega t + n \sum_{\substack{n=6k \pm 1 \\ k=1,2,3}} (-1)^k \frac{1}{n} \sin n\omega t \right] \quad (9)$$

The formula:  $I_d$  is ac side inductor current. Let  $I^* = \frac{2\sqrt{3}I_d}{\pi}$ , here for 20 times less harmonic compensation will yield:

$$\Omega = \frac{3E_m}{\omega C} (a_{11} \sin 6\omega t + a_{12} \sin 12\omega t + a_{13} \sin 18\omega t) - \frac{3L}{C} (a_{21} \cos 6\omega t + a_{22} \cos 12\omega t + \dots + a_{26} \cos 36\omega t) \quad (10)$$

Collating from equation (10), we have:

$$\Omega \approx \sqrt{\left(\frac{-3E_m}{\omega C} a_1\right)^2 + \left(\frac{3L}{C} a_2\right)^2} \sin(6\omega t + \varphi) \quad (11)$$

Where  $a_1 = -0.0095I^*$ ,  $a_2 = -0.0386(I^*)^2$ .

Through the above analysis available DC voltage fluctuation rate is expressed as:

$$\delta \approx \frac{3\sqrt{a_1^2 E_m^2 + a_2^2 \omega^2 L^2}}{2\omega C U_{dc}^2} \quad (12)$$

Thus, it can be seen from the aforementioned equation that under certain conditions, a proper control of the capacitance of DC link voltage can rate the smaller the value of the voltage fluctuation, hence resulting in better compensation effect of APF.

### 3. THE DESIGN OF DC-SIDE OUTPUT VOLTAGE DEVIATION SQUARED VALUE OF FUZZY-PI CONTROLLER

By grain section of the DC side voltage undulation rate equation, based on the DC side voltage ripple and analysis of energy conversion, admiral general traditional DC side voltage deviation value  $\Delta U_{dc}$  as the input amount of PI control will maintain the stability of the DC side voltage. But this method is obviously insufficient, in the process of control since it cannot effectively reduce the no-load current of APF. No-load current will influence the final compensation effect and at the same time, voltage rise time on both ends of the dc side will be slow. Further, it will have negative effect of the dynamic characteristics. Therefore taken the above supposition into consideration, the deficiency of the DC side voltage set point is determined and stability control must be put in place to ensure that the compensation of the shunt active filter effect and also, to ensure its safe and reliable operation. Here, DC voltage deviation squared value is used as the input signal from the controller. The calculation process is shown in equation 13 [16, 17], Where  $U_{ref}$  is as a given reference voltage.

$$\Delta U_{dc}^2 = (U_{ref} - U_{dc}) * |U_{ref} - U_{dc}| \quad (13)$$

After the square of the voltage deviation is determined, its value will be used as inputs fuzzy-PI control, as shown in Fig. (2).

The design method of fuzzy controller is to use the voltage deviation squared value as the error E and the rate of change is EC. Assuming that  $\Delta K_p$  and  $\Delta K_i$  are the fuzzy PI

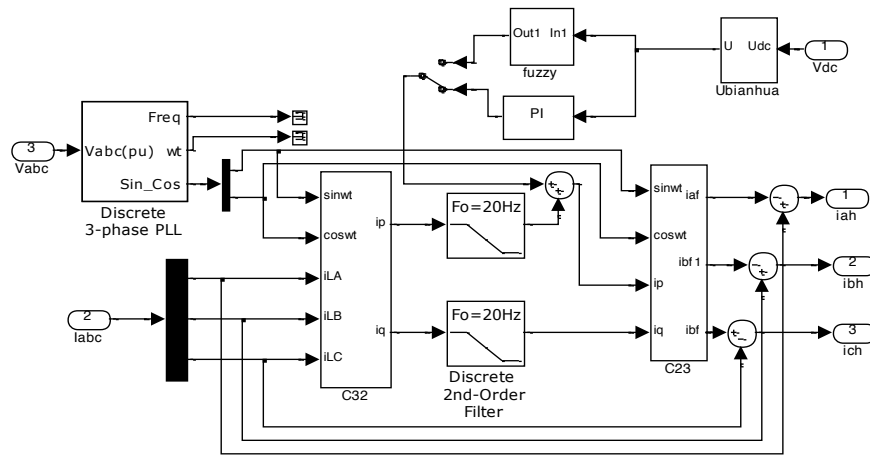


Fig. (3). The current module of system instructions.

Table 1.  $\Delta K_p$  fuzzy control rules.

EC	E						
	PB	PM	PS	ZE	NS	NM	NB
PB	PB	PB	PB	PS	NB	NM	NS
PM	PB	PB	PM	PS	NM	NS	ZE
PS	PB	PM	PS	ZE	NS	ZE	PS
ZE	PM	PS	ZE	ZE	ZE	PS	ZE
NS	PS	ZE	NS	ZE	PS	PM	NS
NM	ZE	NS	NM	PS	PM	PB	NM
NB	NS	NM	NB	PS	PB	PB	NB

controller parameters derived from the correction as a comparative PI controller integral parameter correction [18, 19]. Taking E and EC as the inputs,  $\Delta K_p$  and  $\Delta K_i$  as outputs, selected input and output variables of the fuzzy language domain is taken as [-6,6]. In taking seven languages on the domain variables namely; NB, NM, NS, ZE, PS, PM, PB, representing negative big, negative middle, and negative small, zero \*, positive small, positive middle, positive big. Again, considering the coverage on the theory of domain and sensitivity, stability and robustness principle, the language of the fuzzy language variables values NB and PB will depict s-shaped membership function curve whereas other variable language values will use triangular membership function curve.  $\Delta K_p$  and  $\Delta K_i$  of the membership function curve is shown in Fig. (3).

Enter the amount in accordance with the relationship between output, develop  $\Delta K_p$  and  $\Delta K_i$  and tune parameters of fuzzy control rules as is shown in Table 1 and Table 2.

After a fuzzy controller in real time, calculate  $\Delta K_p$  and  $\Delta K_i$ . Using Center of gravity approach for solving Fuzzy algorithm, the actual value  $\Delta K_p$  and  $\Delta K_i$  after the operation

of Fuzzy solution is used to modify the traditional parameters as indicated in equation (14):

$$\begin{aligned} K_p &= K'_p + \Delta K_p \\ K_i &= K'_i + \Delta K_i \end{aligned} \tag{14}$$

Where:  $K'_p$  and  $K'_i$  are the original setting of good PI parameters,  $\Delta K_p$  and  $\Delta K_i$  are the outputs of Fuzzy controller. Traditional closed loop PI control rely too much on precision of mathematical model of the system, poor robustness. Therefore, in the complex system control system, it is difficult to achieve satisfactory effect. Fuzzy control is to make up for the deficiencies of the original control strategy which will make the system achieve stability quickly thereby reducing the overshoot and switching load current shock and also, keep the integral part of PI control's ability to solve system steady-state error. Fig. (3) shows the current module of system instructions.

In Fig. (3),  $i_{ah}$ ,  $i_{bh}$  and  $i_{ch}$  are harmonic currents by  $i_p - i_q$  detection method which is compensated by generating a PWM pulse signal generated by the voltage control signal to control the opening of the switching device off. General ap-

Table 2.  $\Delta K_i$  fuzzy control rules.

EC	E						
	PB	PM	PS	ZE	NS	NM	NB
PB	NB	NB	PM	PB	PM	PS	ZE
PM	NB	NB	PS	PB	PS	ZE	NS
PS	NB	NM	ZE	PM	ZE	NS	NM
ZE	NM	NM	NS	ZE	NS	NM	NM
NS	NM	NS	ZE	PM	NM	NM	NB
NM	NS	ZE	PS	PB	NM	NB	NB
NB	ZE	PS	PM	PB	NB	NB	NB

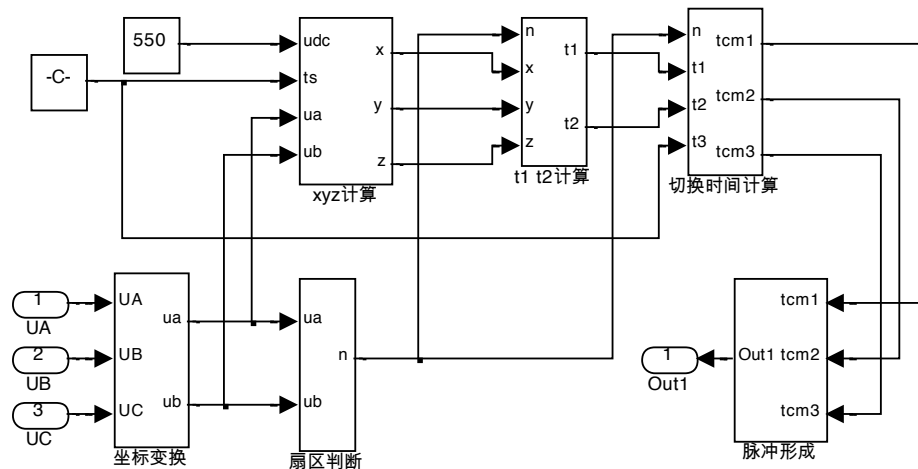


Fig. (4). The simulation model diagram of SVPWM.

proach is to use a triangular carrier control and hysteresis control. When triangular carrier control following error is large, the switching loss is also large. Hysteresis control will result in a larger pulse, so in order to reduce the DC voltage ripple, SVPWM modulation strategy is used. Space vector pulse width modulation (SVPWM) in the APF is a very effective PWM control techniques [20-22]. Space vector pulse width modulation voltage space vector contains six equal amplitudes ( $2U_{dc}/3$ ), Phase difference  $60^\circ$  electrical angle of zero vector  $U_1 - U_6$ . This six vectors in the complex plane are divided into six sectors, located in the center of the complex plane amplitude is zeros' zero vector  $O_0$  and  $O_7$ . The use of a linear combination of SVPWM control strategy to control switch between two adjacent nonzero vector ( $U_{60}$  and  $U_{120}$ ) and zero vector ( $O_0$  and  $O_7$ ) make each control period to approximate the continuous rotation of the reference vector  $U_{ref}$  [23-25].

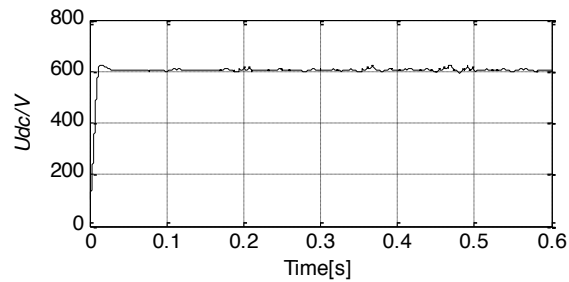
When the reaction time of two nonzero vector synthesis output vectors are equal and the role of time zero vector is zero, the space vector pulse width modulation method can

achieve the minimum DC voltage utilization. At any time of Active Power Filter output, vector angle and amplitude of the output voltage is determined by the power grid voltage drop compensation loop vector and the vector sum of the decision [26, 27]. Therefore, any time DC voltage utilization gets the most hours, minimum value can be determined to meet the required DC side capacitor in order to reduce the DC voltage ripple. Fig. (4) is a diagram for the simulation model.

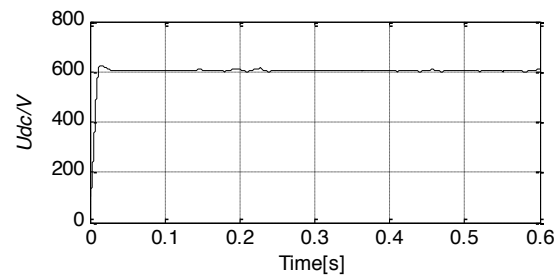
#### 4. SIMULATION STUDY

In order to verify whether the above methods are reasonable, we use MATLAB / SIMULINK to simulate it. Three-phase voltage supply of circuit simulation is 380V/50Hz, non-linear load resistance  $R=30\ \Omega$ ,  $L=10e-3H$ , APF module AC side resistance  $R=0.02\ \Omega$ ,  $L=2mH$ , inverter DC capacitor value is  $C=6800\ \mu F$ , given voltage value  $U_{ref}=600V$ .

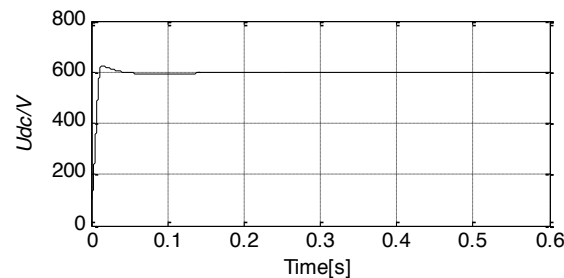
For comparison control effect, we set switch module in Fig. (3), so as to switch between fuzzy PI control and simple PI control. Simulation results Pictured DC voltage value  $U_{dc}$ , where figure (a) is a direct result of the simulation PI con-



(a) The traditional PI control



(b) Deviation of the traditional PI control



(c) Deviation of the fuzzy-PI control

**Fig. (5).** Capacitance value is 6800uF.

troller, figure (b) is the simulation results after selecting the square of the voltage deviation as a PI controller input signal, figure (c) is the simulation results added to the square of the voltage deviation as fuzzy-PI controller input signal, as is shown in Fig. (5).

After simulation, it was found out that there is obvious current ripple in the use of simple and conventional PI controller. When the square of the voltage deviations is used as conventional controller, the DC voltage ripple is reduced significantly, but it still exists. However, when square of the voltage deviations is used as the fuzzy PI controller, it was ascertained that the voltage is equal to the given voltage and the ripple is greatly reduced.

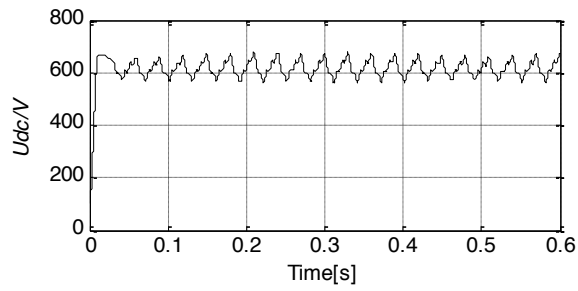
In order to better illustrate the simulation results, the capacitance values selected here were 10000uF and 4700uF to compare the simulation results, as is shown in Figs. (6 and 7).

The simulation results show that when the capacitor value is selected 4700uF, DC voltage fluctuation rate is large. Measured the data from the simulation diagram, the voltage value is from 590.8v to 619.2v by using traditional PI method, it is from 600.4v to 610.7v by adopting the deviation of

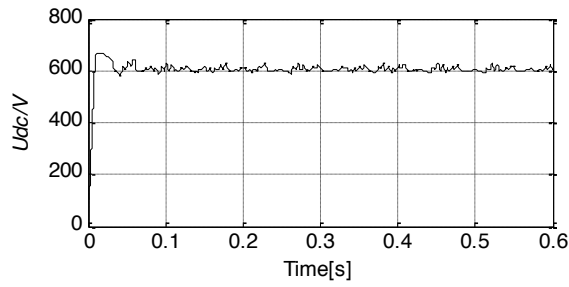
traditional PI method. The voltage value from 640V decreased to 590V after reaching the given voltage value 600V if by using the deviation of fuzzy PI method. Obviously, the capacitance value is too small to lead to the waveform is very unstable. When 10000uF of the capacitance value is selected, DC voltage ripple is small, maximum ripple voltage is 610v by using traditional PI method whilst maximum ripple voltage is 603v by adopting the deviation of traditional PI method. When using the deviation of fuzzy PI method, the ripple voltage and the impulse voltage disappear and the voltage value is directly proportional to the given voltage 600v. According to the simulation results and considering the actual application, choosing 6800uf DC voltage for capacitor, the voltage values are faster, tend to be stable and lead to elimination of ripple components.

## 5. EXPERIMENTAL VERIFICATION

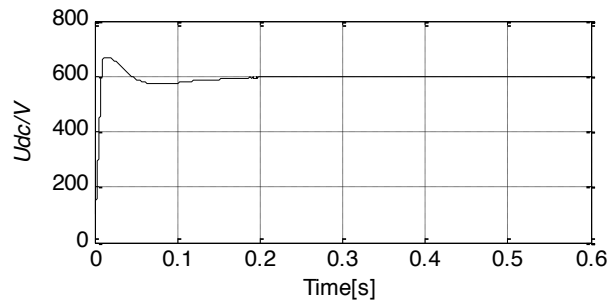
The experiment is based on 380V/66KVA APF prototype. Experimental conditions: Three-phase AC voltage is 380V/50Hz, the IGBT switching frequency is 6.4 kHz, nonlinear load resistance is 30  $\Omega$ , inductance value is 10mH,



(a) The traditional PI control

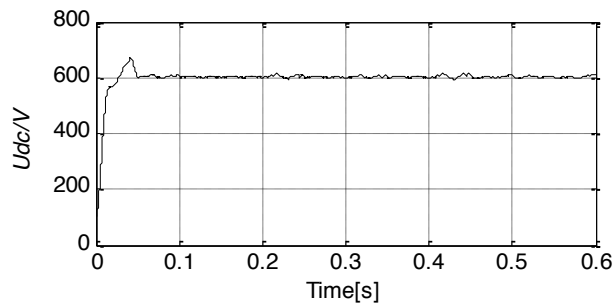


(b) Deviation of the traditional PI control

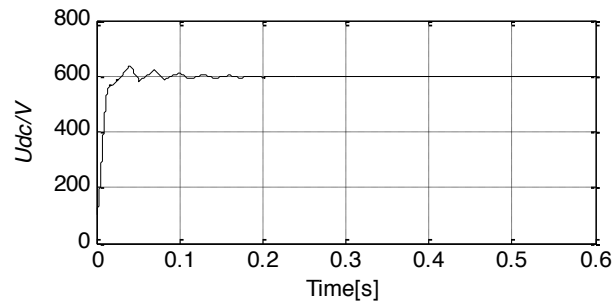


(c) Deviation of the fuzzy-PI control

Fig. (6). Capacitance value is 4700uF.

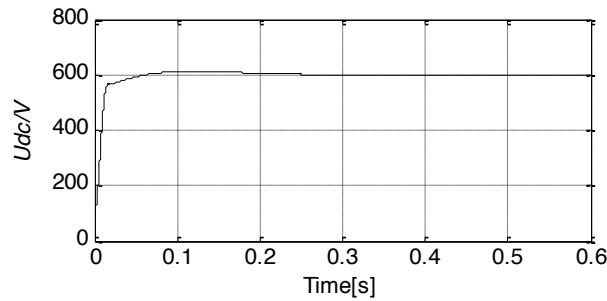


(a) The traditional PI control



(b) Deviation of the traditional PI control

Fig. (7). Contd...



(c) Deviation of the fuzzy-PI control

Fig. (7). Capacitance value is 10000uF.

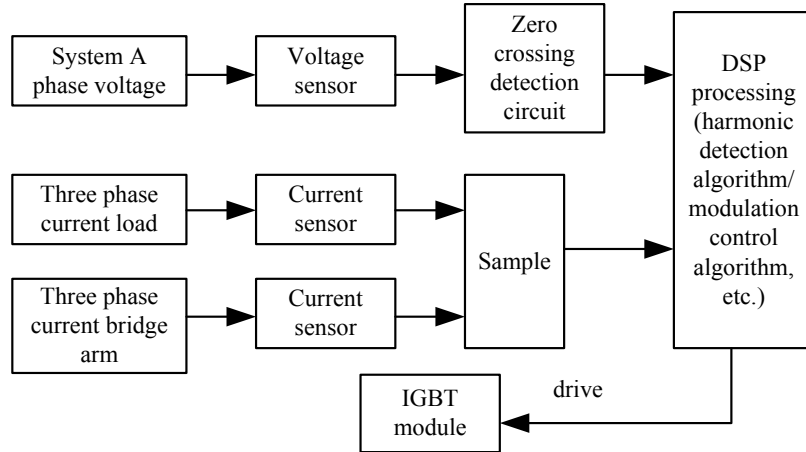


Fig. (8). System control block diagram of a three-phase shunt APF.



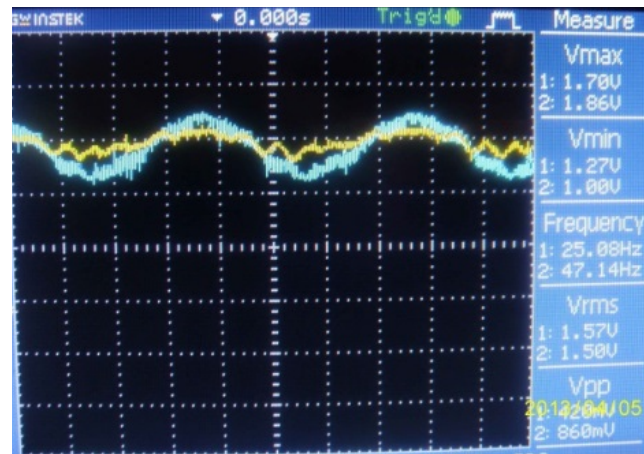
Fig. (9). APF prototype and nonlinear load.

inverter dc side capacitor value is 6800uF, DC side given voltage value is 650V. Control links adopt the deviation of Fuzzy - PI regulating method, harmonic detection algorithm uses the  $i_p - i_q$  detection method based on the theory of instantaneous reactive power and the current tracking control uses modulation method based on space vector pulse width. Three-phase shunt APF control system block diagram is shown in Fig. (8). Three-phase load current, bridge arm current and DC side voltage signal through the sensor meas-

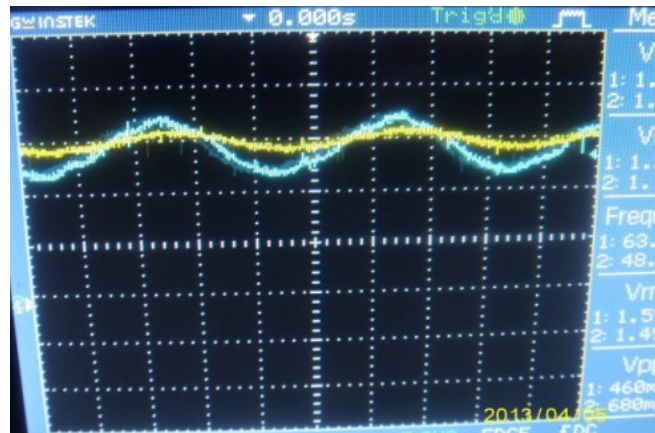
urement circuit into A/D conversion chip to sample, sampling chip uses the AD574A. This is experimented by using deviation Fuzzy - PI control method to reduce the DC voltage ripple.

As shown in Fig. (9) for the physical prototype and nonlinear load harmonic source.

Fig. (10) depicts the supply voltage waveforms (blue line) and DC side capacitor voltage waveform (yellow line) comparison chart.



(a)



(b)

**Fig. (10).** Experimental waveforms.

Fig. (10a) is the traditional PI control method. The waveform tends not to be smooth due to the present of ripple.

Fig. (10b) is the deviation of Fuzzy - PI control. The waveform is improved in full compliance with the system to eliminate the DC voltage ripple requirements.

As seen from the experimental results, in the use of voltage deviation square values of Fuzzy -PI controller, DC side voltage ripple is very small and almost stable. The stable voltage waveform is to achieve a given voltage 650v. Adopting the square voltage deviation value as the input signal of fuzzy PI controller-PI controller can effectively improve the DC side voltage ripple.

## CONCLUSION

Through MATLAB simulation and APF prototype experiment, it can be found out that DC capacitor directly affects the efficiency of the APF but current measurements are influenced by the DC side capacitor ripple voltage. In addition, Adopting DC-side output voltage deviation squared value of fuzzy-PI control method as voltage control and also, adopting SVPWM as pulse width modulation can effectively solve the problem of DC side ripple voltage and achieve the purpose of the stability of the desired dc side voltage.

## CONFLICT OF INTEREST

The authors confirm that this article content has no conflict of interest.

## ACKNOWLEDGEMENTS

This project was supported by the Nature Science Foundation of Gansu Province (No. 1308RJYA044) and Scientific Research Project in Gansu Province Department of Education (2014-045).

## REFERENCES

- [1] F.H. Juan, "A study on the DC voltage control techniques of cascaded multilevel APF", *Int. Power. Electron. Motion. Control. Conf.*, vol. 4, pp. 2727-2731, 2012.
- [2] L. Zhan-Ying, R. Zhen, and Y. Ze-ming, "Survey on active power filter devices and their application study", *Power. Syst. Technol.*, vol. 28, no. 22, pp. 40-43, 2004.
- [3] L. Jian, and Kai-pei, "Parameters optimization method of three-phase four-wire shunt active power filter based on unified mathematical model", *Trans. China Electrotech. Soc.*, vol. 27, no. 10, pp. 220-227, 2012.
- [4] W. Zhu, R. Fan, and K. Zhou, "Study on a novel hybrid active power filter applied to a high-voltage grid", In: *IEEE Trans. Power Deliv.*, 2009.

- [5] D. Xu, and H. Fang, "Active power filter with optimal dc side condenser", In: *IEEE Symp. Bus. Eng. Ind. Appl.*, pp. 7-12, 2012.
- [6] X. Huang, J. Liu, and H. Zhang, "A simplified shunt APF model based on instantaneous energy equilibrium and its application in DC voltage control" In: *Power. Electron. Spec. Conf.*, pp. 2235-2241, 2008.
- [7] F. Briz, P. Garcia, and M.W. Degner, "Dynamic behavior of current controllers for selective harmonic compensation in three-phase active power filters", *IEEE. Trans. Ind. Appl.*, vol. 49, no. 3, pp.1411-1420, 2013.
- [8] F. Ma, and A. Luo, "Voltage ripple analysis of simplified active power compensator for negative sequence and reactive power compensation", In: *IET. Power. Electron.*, pp. 2582-2594, 2014.
- [9] L. Török, L. Mathe, and S. Munk-Nielsen, "Voltage ripple compensation for grid connected electrolyser power supply using small DC link capacitor", *Int. J. Elec. Power Energy Syst.*, vol. 38, no. 2, pp. 607-611, 2014.
- [10] A. Munduate, I. Garin, E. Figueres, and G. Garcera, "Analytical study of the DC link capacitors voltage ripple in three level Neutral Point Clamped Inverters", In: *Power Electron. Elec. Drive. Auto. Motion.*, 2006, pp. 552-555.
- [11] W. Xue-liang, D. Ke, and K.Yong, "A parallel control strategy of three-phase three-wire shunt active power filters", *Autom. Elec. Power. Sys.*, vol. 31, no. 1, pp. 70-74, 2007.
- [12] L. Asiminoaei, C. Lascu, and F. Blaabjerg, "Performance improvement of shunt active power filter with dual parallel topology", *IEEE. Trans. Power. Electron.*, vol. 22, no. 1, pp. 247-259, 2007.
- [13] N. Zaveri, and A. Chudasama, "Control strategies for harmonic mitigation and power factor correction using shunt active filter under various source voltage conditions", *Int. J. Elec. Power Energy Syst.*, vol. 42, no. 1, pp. 661-671, 2012.
- [14] H. Dogan, and R. Akkaya, "A simple control scheme for single-phase shunt active power filter with fuzzy logic based DC bus voltage controller", *Lect. Notes Eng. Comp. Sci.*, vol. 2175, pp. 1505-1509, 2009.
- [15] H. Na, W. Jian, and X. Dianguo, "Fuzzy control of DC voltage in active power filter", *Power. Syst. Technol.*, vol. 30, no. 14, pp. 45-48, 2006.
- [16] H. Wei, Z. Zhi-dan, and Z. Yi-hui, "Repeat PI controller based on neural network phase shunt active power filter", *Power. Syst. Protect Control.*, vol. 40, no. 3, pp. 78-84, 2012.
- [17] G. He-rong, W. De-yu, S. Hong, Z. Wei, and G. Xiao-qiang, "Technology research of three-phase four-leg inverter control", *Power Syst. Protect. Control.*, vol. 39, no. 24, pp.41-46, 2011.
- [18] K. Jains, P. Agrawal, and HO. Gupta, "Fuzzy logic controlled shunt active power filter for power quality improvement", *IEE. Proc. Electr. Power Appl.*, vol. 149, no. 5, pp.317-328, 2002.
- [19] W. Chonglin, M. Caoyuan, and L. Dechen, "Study on improved neural network pid control of APF DC voltage", *Innov. Manag. Ind. Eng.*, vol. 62, pp. 179-182, 2009.
- [20] Q. Geng, C. L. Xia, Y. Yan, and W. Chen, "Direct power control in constant switching frequency for PWM rectifier under unbalanced grid voltage conditions", *Proc. Chin. Soc. Electr. Eng.*, vol. 30, no. 36, 79-85, 2010.
- [21] H. Li, K. Zhang, and H. Zhao, "Active DC-link power filter for single phase PWM rectifiers", In: *8<sup>th</sup> Int. Conf. Power Electron.*, 2011.
- [22] O.V.S.R. Varaprasad, and D.V.S.S.S Sarma, "An improved SVPWM based shunt active power filter for compensation of power system harmonics", In: *IEEE. 16<sup>th</sup> Int. Conf.*, 2014, pp. 571-575.
- [23] S. Masjedi, and Hr. Najjar, "Designing distribution networks for omitting harmonics based on SVPWM using ANN for APF", In: *Electr. Power. Distrib. Netw.*, 2012, pp.1-7.
- [24] G. Panda, S.K Dash, and N. Sahoo, "Comparative performance analysis of shunt active power filter and hybrid active power filter using FPGA-based hysteresis current controller", In: *IEEE 5<sup>th</sup> India. Int. Conf. Power Electron. (IICPE).*, 2012, pp. 1-6.
- [25] S. Garlapati, and R. Gupta, "Shunt active power filter as front end converter for DC loads Power Electronics", In: *IEEE 5<sup>th</sup> India. Int. Conf. Power. Electron. (IICPE).*, 2012, pp. 1-6.
- [26] Z. Bin, W. Danwei, and Z. Keliang, "Linear phase lead compensation repetitive control of a CVCF PWM inverter" *IEEE. Trans. Ind. Electron.*, 2008, vol. 55, no. 4, pp.1595-1602.
- [27] R. Grino, R. Cardoner, and C. Castello, "Digital repetitive control of a three-phase four-wire shunt active filter", *Ind. Electron. IEEE. Tran.*, 2007, vol. 57, no. 3, pp. 1495-1503.

Received: June 09, 2014

Revised: June 22, 2015

Accepted: July 24, 2015

© Wu et al.; Licensee Bentham Open.

This is an open access article licensed under the terms of the Creative Commons Attribution Non-Commercial License (<http://creativecommons.org/licenses/by-nc/3.0/>) which permits unrestricted, non-commercial use, distribution and reproduction in any medium, provided the work is properly cited.